Investigation on Dynamics of the Flow Control Unit in Ventilator Systems and its Fundamental Performance Limitations

Yufeng Li PhD, Member IEEE, VIASYS HealthCare. Yorba Linda, CA

yufeng.li@viasyshc.com

Abstract

In the design of a flow servo for critical care ventilator systems, control engineers are often troubled by unwanted oscillations or instability problems since these devices are typically operated under a wide variation conditions. Without knowing the dynamic behavior and its fundamental limitations of the flow control unit in ventilators, even ad-hoc extensions to standard PI control, as usually done in practice, is not able to solve all the problems and satisfy the overall performance required. In this paper, through analytical modeling and experimental identification, the root of the control problem is investigated by analyzing the dynamics of the flow control unit. Here the so called flow control unit includes a type of solenoid operated flow control valve and its exit manifold. A controller is designed by using model linearization methods, and the fundamental control limitation of the flow control unit is examined.

1. Nomenclature

a_d	Cross-sectional area of the diaphragm
a_s	Cross-sectional area of the valve seat
A_0	Geometric orifice of the valve
b	Damping coefficient of the valve
C_d	Discharge coefficient
C	Patient circuit compliance
D	Diameter of the seat
F_{mag}	Solenoid magnetic force
F_{s0}	The sum of the preload spring force
g	Acceleration due to gravity
k_s	Spring constant of the valve
k_e	Electronic-force gain
k_{dc}	DC gain of the transfer function
k_u	Valve static characteristics
m	Mass of the valve poppet
p_a	Atmosphere pressure
p_1, p_2	Valve inlet and outlet pressures
p_{1a}, p_{2a}	Valve inlet and outlet absolute pressures
p_b	Backpressure
q	flow rate
R	Patient circuit resistance
T_1	Temperature
u	Control input/ voltage input to valve solenoid
x	Poppet position
γ	A specific heat ratio of gas mixture.

2. Introduction

Patients who need breathing assistance are usually placed on mechanical ventilation. Based on the setting predetermined by clinicians, a system of flow delivery and exhaust valves provide cyclic control of either pressure or volume to maintain adequate ventilation of the patient's lungs. In ventilator control systems, delivery of flow is the key part for any type of breath assistance. A stable, fast response, high accuracy flow servo is then typically required for supplying the desired breathing gas to patients. This requirement is even more stringent for ventilators applied to infant and neonatal patients. PI control is normally used in ventilator flow servo systems, however control engineers are often troubled by unwanted flow oscillations or instability problems when the ventilator is operated under different conditions. Typically, an ad-hoc tuning method has to be used, but in many cases the method does not solve the problem. Moreover it makes the control implementation more and more complex and difficult to maintain/trace. In order to design a high performance flow servo, understanding not only the valve nonlinearity but also the dynamics of the whole flow control unit becomes an important issue for control engineers.

The dynamics of the flow control unit mainly depends on the dynamics of the flow control valve (FCV). However, it must be also aware that the exit manifold of the FCV may also affect the FCV dynamics significantly. Through analytical modeling and experimental identification, this paper studies the nature of the dynamics and performance limitations of the ventilator flow control unit. The rest of the paper will be arranged as follows: In section 3, following a briefly describing the flow unit configuration, the linear model for the FCV is derived. In section 4 the model is identified and validated by frequency domain and time domain methods based only on input and output measurements, the effect of the valve exit manifold is also examined. Then model linearization and controller design is

presented in section 5. The performance limitations are analyzed in section 6. Finally the conclusion is given in section 7.

3. System description and FCV modeling

The gas flow in critical care ventilation systems is controlled by a FCV. A flow sensor connected to the FCV outlet provides the actual information of the inspiratory flow for closed loop control. The gas is then delivered to the patient through a safety/relief valve and outlet manifold. Figure 1. shows the sketch of the flow control unit.

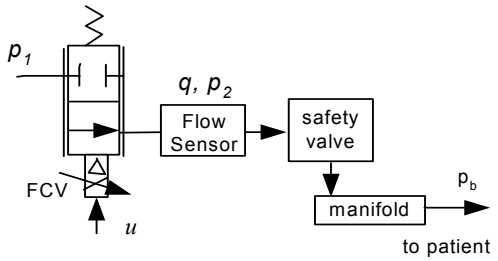

Figure 1. Flow control unit

The FCV used in the ventilator is a normally closed, two-way solenoid operated valves. It is also referred as proportional valves since the displacement of the valve poppet is proportional to the applied current. The magnetic and electric components are isolated from the working medium by a diaphragm. For reducing the friction effect, the armature of the valve is suspended between a pair of thin, flat springs in order to eliminate metal-to-metal contact. The preload spring force generated by the upper spring and the two flat springs provides the necessary seating force to preclude seat leakage when the valve is de-energized.

The modeling of the FCV can be separated into three parts. The solenoid itself is governed by general rules of electro-magnetic circuits, the mechanical part of the poppet is expressed by a spring-mass system and the fluid flow property is described by a sufficiently accurate orifice equation.

- *Solenoid force*

Modeling and analysis of the electro-magnetic circuit for a solenoid valve is usually quite complex, it involves several intermediate states, e.g., current, flux linkage and poppet position. The detail model of different types of solenoid valve can be found in open literature, for example [1] and [2]. In general, depending on the specific mechanical and electrical components, as well as the desired closed loop speed of the motion control, the electro-magnetic dynamics may or may not be comparable to mechanical dynamics. The electro-magnetic dynamics can usually be improved by using current feedback in the motion control loop, thus to reduce the effects of resistance, reluctance, inductance and back emf in the solenoid circuit. This is out of the scope of this paper. For simplification, here the relation between the electrical input and magnetic force output is presented by a static nonlinear gain k_e,

$$F_{mag} = k_e u \tag{1}$$

- *The poppet motion equation*

The magnetic flux developed in the solenoid core applies a force on the poppet, resulting in the poppet displacement. The motion of the poppet can be simply described by a force balance equation:

$$m\ddot{x} + b\dot{x} + k_s x = k_e u - F_{s0} - a_s(p_{1a} - p_{2a}) + a_d p_{1a} \tag{2}$$

where $p_{1a} = p_1 + p_a$, $p_{2a} = p_2 + p_a$. For the valve design considered here, the cross-sectional area of the diaphragm is made equal to the seat area, i.e., $a_s = a_d$, the net force produced by the inlet pressure on the poppet is zero. So the linearized transfer function of equation (2) is:

$$(ms^2 + bs + k_s)\delta x = k_e \delta u + a_s \delta p_2 \tag{3}$$

- *The equation of mass flow*

The flow equations can be described accurately enough by the orifice equation [3].

$$q = C_v(p_{1a,} p_{2a}) A_0(x) = C_v(p_{1a,} p_{2a}) \cdot \pi D x \tag{4}$$

where $A_0(x) = \pi D \cdot x$ if $x \le D/4$.

$$C_v(p_{1a,} p_{2a}) = p_{1a} C_d \sqrt{\frac{2\gamma g}{T_1(\gamma - 1)}} \left[\left(\frac{p_{2a}}{p_{1a}} \right)^{\frac{2}{\gamma}} - \left(\frac{p_{2a}}{p_{1a}} \right)^{\frac{\gamma+1}{\gamma}} \right]^{\frac{1}{2}}$$

C_v depends on gas properties, temperature T_1 and is a function of $p_{2a}/p_{1a.}$ Assuming that the upstream pressure p_{1a} and the temperature T_1 are constant, the nonlinear flow equation (4) can be linearized with respect to x and p_2:

$$\delta q = \alpha \delta x + \beta \delta p_2 \tag{5}$$

$$\alpha = \left. \frac{\partial q}{\partial x} \right|_{p_{1a,} p_{2a0,} x_0} = C_v(p_{1a,} p_{2a,0}) \pi D$$

$$\beta = \left. \frac{\partial q}{\partial p_{2a}} \right|_{p_{1a,} p_{2a0,} x_0}$$

$$= p_{1a} \left(\frac{C_v(p_{1a,} p_{2a,0})}{r p_{2a,0}} - \frac{p_{1a} g}{T R C_v(p_{1a,} p_{2a,0})} \cdot \left(\frac{p_{2a,0}}{p_{1a}} \right)^{1/r} \right) \pi D x_0$$

The subscript '0' denotes that the linearization is done around a nominal operating point. The linear model of

the valve is illustrated in Figure 2.

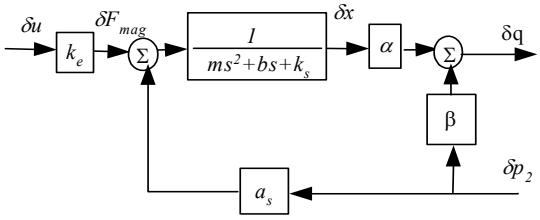

Figure 2. Linearized model of FCV

Mathematically, the output flow is described by

$$\delta q = \frac{k_e \alpha}{ms^2 + bs + k_s}\delta u + \frac{\beta(ms^2 + bs + k_s + a_s\alpha/\beta)}{ms^2 + bs + k_s}\delta p_2 \tag{6}$$

In summary, the flow valve dynamics primarily come from the poppet motion. The variation of the downstream pressure p_2 can be regarded as a perturbation to the orifice flow. The sensitivity to p_2 effect is determined by the valve design parameters a_s and β.

4. Model identification and validation

To validate the FCV model derived in the previous section, a frequency domain identification method is used to obtain the linear transfer function of FCV, i.e., from input u to the valve output flow q directly. To do this, the FCV is first separated from the flow control unit shown in Figure 1, a high performance flowmeter TSI is connected to the FCV outlet and its downstream is open to air pressure so that $p_2 \approx 0$.

In the identification experiments, a random binary voltage signal with a frequency band of [0, 250Hz] is applied to the FCV. The signal is generated by the MATLAB function 'idinput', and is broken into 5 periods (M=5), each period contains N=2048 points. The reason for using a periodic input signal is to avoid the distortion resulting from nonlinear and noise effects [4]. The signal variation magnitude is around 1.0v. Operating points corresponding to flow range from 1.4 to 72 LPM have been tested. 2ms sampling time is used in the experiments.

Averaging the measurements over the repeated periods for each test, the frequency response from input u to output flow q is obtained as shown in Figure 3. The frequency responses are then fitted by the following transfer function,

$$G(s) = \frac{q(s)}{u(s)} = \frac{k_{dc}G_{fcv}(s)e^{-0.003s}}{0.004s+1} \tag{7}$$

The first order transfer function with 3ms time delay correspond to the TSI dynamics. So the transfer function of the FCV is actually $k_{dc}G_{fcv}(s)$, where k_{dc} is a nonlinear DC gain depending on the valve static characteristics at each operating condition, and

$$G_{fcv}(s) = \frac{1}{s^2/\omega_n{}^2 + 2\zeta_n/\omega_n\, s + 1} \tag{8}$$

It describes the resonant mode associated with the poppet motion dynamics, where ω_n=170Hz and ζ_n=0.1 have been identified for all the operating points.

The same experiments are then applied to the ventilator flow control unit shown in Figure 1. Now the flow data is measured by the built in flow sensor, and the tested flow range varies from 5 to 120 LPM. The obtained frequency responses are plotted in Figure 4 and can be modeled by the following structure,

$$\begin{aligned} G(s) &= k_{dc}G_p(s) \\ &= k_{dc}\frac{s^2/\omega_0{}^2 + 2\zeta_0/\omega_0\, s + 1}{s^2/\omega_n{}^2 + 2\zeta_n/\omega_n\, s + 1}\cdot\frac{e^{-0.004s}}{0.006s+1} \end{aligned} \tag{9}$$

Compare with the model (7), we see that besides the mechanical resonant mode of the FCV and the new sensor dynamics, a pair of conjugate complex zeros appearing in the numerator determines the dynamic contribution from the downstream components. It is observed that the pressure p_2 at the valve outlet varies during the frequency response tests. In other words, the second term of (6) has considerable contribution to the frequency responses of the valve. Since the system has only one control input *u*, the changing in p_2 is actual the pneumatic result of the changing in *u*. Therefore, the transfer function of the whole flow control unit is then described by $k_{dc}G_p(s)$. The locations of the conjugate zero depend on the operating conditions. As it is found in the experiments, the operating points change from 5 to 120 LPM, ω_0 moves from 65Hz to 85Hz and ζ_0 is so small that can be neglected. The two lines in Figure 3 and Figure 4 plotted with "-o-" are the model fittings to the measured frequency responses of the lowest and the highest operating points.

For the whole operating range, the model of the flow control unit can be characterized by the two separate parts, in terms of the static and dynamics behaviors, as shown in Figure 5. The dynamics is described by $G_p(s)$ which is a family of linear transfer functions; the static gain k_{dc} lumps the nonlinear properties of both electro-magnetic and orifice flow equation. Actually the valve static characteristics can be described by $k_u = k_{dc}(u - u_0)$. $u_0 = (F_{s0} - p_a a_s)/k_e$ is the offset produced by the preload force F_{s0} and the force from ambient pressure p_a since p_a acts only on the poppet

downstream side. k_u can be identified by commanding the FCV with an incremental/decremented voltage signal. With each step having a 1 second duration, and measuring the output steady-state flow, the curve of q vs. u is obtained and u_0 is identified around 1.4 volt as shown in Figure 6.

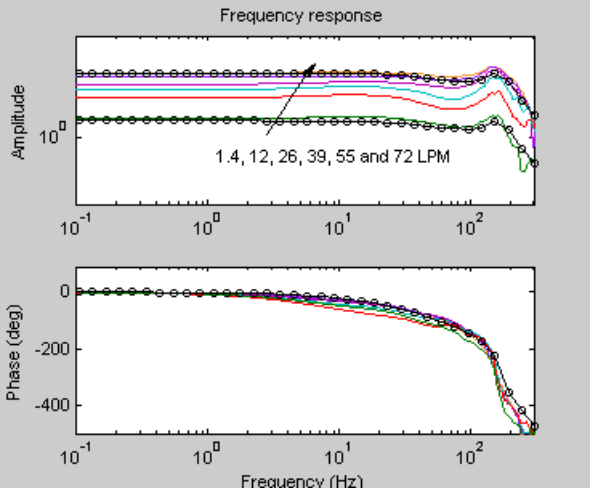

Figure 3. Frequency response of the FCV, measured by TSI.

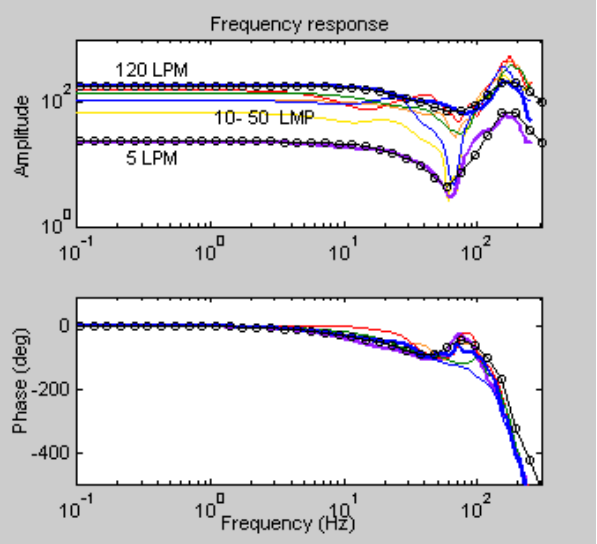

Figure 4. The frequency response of the flow control unit in the ventilator at different operating points.

Note that the valve static characteristics curve is obtained with zero p_b. In the cases of the backpressure $p_b \neq 0$, the effect of p_b is equivalent to decreasing u_0 or moving the static curve of the valve to the left. To separate the backpressure effect from the measured valve static characteristics, a constant k_f is introduced in the model that takes into account the effect of p_b, as shown in Figure 5. k_f is also nonlinear depending on the operating point. The average value of k_f is about 0.45.

Figure 7 and Figure 8 show the time domain fitting with and without backpressure disturbance; in both cases, the input voltage is a square wave.

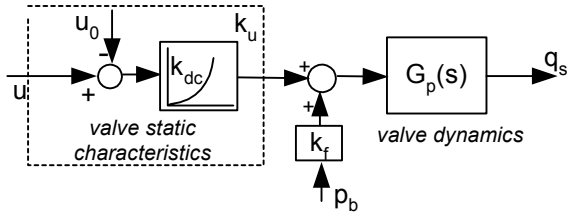

Figure 5. The model of the flow control unit

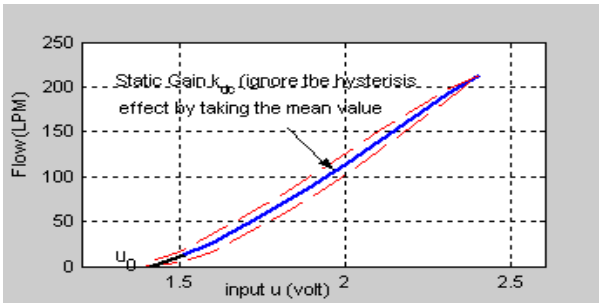

Figure 6. The static characteristics of the FCV

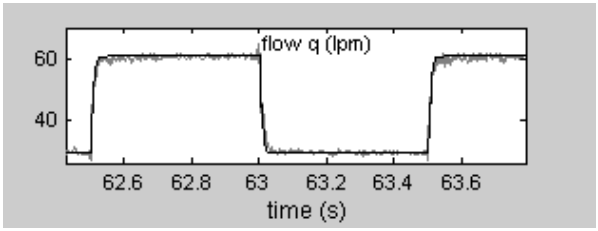

Figure 7. The time response of the output flow without backpressure disturbance, model (black), real (gray).

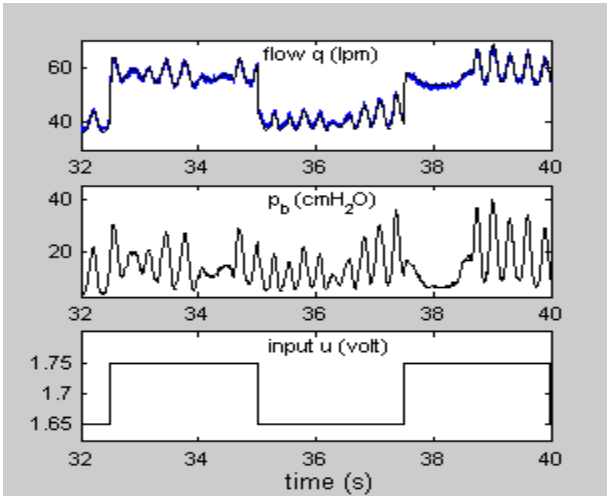

Figure 8. The time response of the output flow with backpressure disturbance, model output (black) and real output (gray).

5. Controller design

Since the valve nonlinear characteristics k_u is already known, the valve can be simply linearized by inversing the valve characteristics. That is, by adding the inversed nonlinear function $\hat{k}_u^{-1}$ in front of the valve, as shown in Figure 11. The virtual linearized flow control unit can be described by $\hat{k}_u^{-1} k_u G_p(s)$. If the inverse is exact, $\hat{k}_u^{-1} k_u = 1$. Without the backpressure disturbance, the linearized plant is simply $G_p(s)$. For this case it is easy to design a PI controller for this linear plant.

6. Analysis for performance limitation

- *The dynamics induced by the effects of the valve exit manifold limit the closed loop bandwidth*

It is found in practice that the closed-loop bandwidth of the flow servo is at least an order of magnitude lower than the natural frequency of the FCV. To understand why, examining the frequency response plotted in Figure 4, we can see that the pair of conjugate zeros induced by the FCV exit manifold results a drastic phase shift. Due to this drastic phase shift, together with actuator saturation, experience shows that, with a conventional PI controller, it is usually not possible to achieve a closed-loop bandwidth higher than 1/5 to 1/3 of the frequency determined by the zeros.

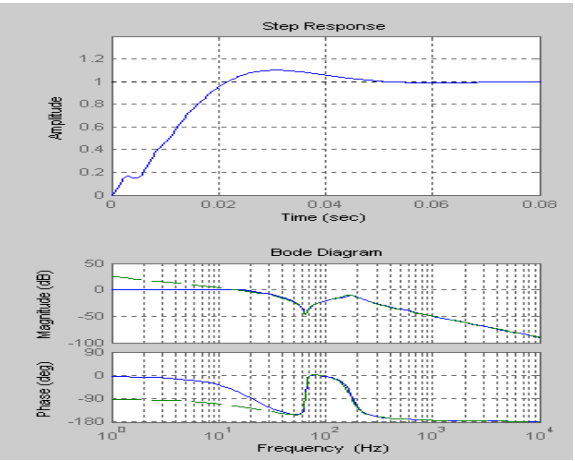

Figure 9. The step response and the bode diagrams (open-loop: dashed, closed-loop: solid line).

This is also approved by simulation. Assuming an operating point at ω_0=65Hz, using an integral control, the control bandwidth can only reach up to around 14Hz if less than 10% overshoot is desired. Figure 9 shows the step response and the bode plots (open-loop: dashed, closed-loop: solid line).

- *Increasing load resistance or decreasing load compliance may induce internal instability into the system*

In the ventilator, the flow servo is connected to the patient circuit for delivering flow to the patient's lungs. Using a simple RC circuit to model the patient[5], the backpressure p_b can be calculated by

$$p_b = (R + \frac{1}{Cs})q \qquad \textbf{(10)}$$

Recalling Figure 5, the output flow is

$$q = (k_u u + k_f p_b) G_p(s) \qquad \textbf{(11)}$$

Inserting (10) into (11), the process transfer function (including the patient circuit) becomes

$$G_{\bar{P}}(s) = \frac{q(s)}{u(s)} = \frac{k_u G_p(s)}{1 - k_f (R + 1/Cs) G_p(s)} \qquad \textbf{(12)}$$

Since the achievable control bandwidth (14Hz) is much lower than the resonance, the analysis can be simplified by approximating the dynamics model $G_p(s)$ with the first order transfer function, $G_p(s) \approx \frac{1}{0.008s + 1}$. This simplified model is able to describe the flow control unit dynamics accurately up to 30Hz, as shown in Figure 10.

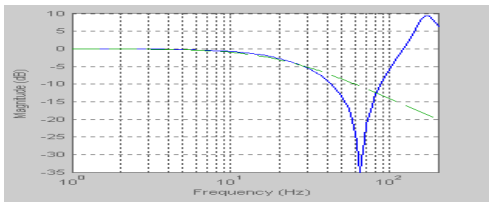

Figure 10. $G_p(s)$ (solid line) and its first order approximation (dashed line).

In this frequency range, we have

$$G_{\bar{P}}(s) = \frac{s}{0.008s^2 + (1 - k_f R)s - k_f / C} \qquad \textbf{(14)}$$

The poles of $G_{\bar{P}}(s)$ are

$$p_i = -\frac{1}{2}(1 - k_f R) \pm \frac{1}{2}\sqrt{(1 - k_f R)^2 + 0.032 k_f / C}$$

Since $\sqrt{(1 - k_f R)^2 + 0.032 k_f / C} \geq (1 - k_f R)$.

as the compliance decreases $C : \infty \to 0$, one of the poles will move from the origin to positive infinity. This means that $G_{\bar{P}}(s)$ is a non-minimum phase system with a right half plane (RHP) pole.

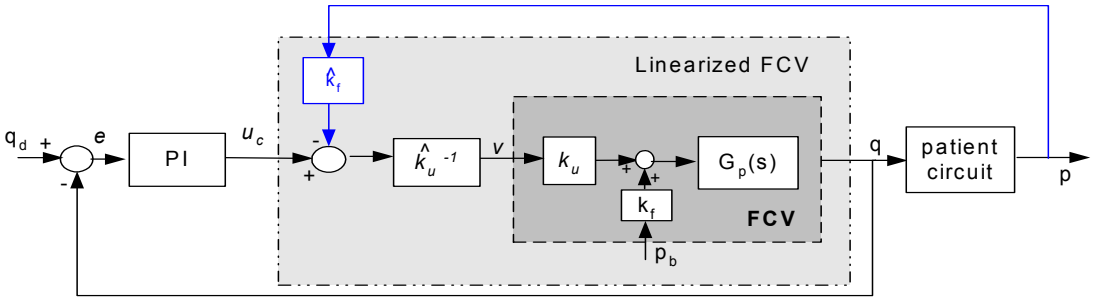

Figure 11. Control block diagram

To stabilize this system, a relative high bandwidth (ω_B>2p) controller is required [6], where p is the frequency of the RHP pole. However, as described in the previous problem, the zeros induced by the downstream pressure limits the achievable bandwidth. When these two required bandwidths approach each other, the system becomes very difficult to stabilize. To solve this instability problem in the controller design, a backpressure compensation term, $-\hat{k}p_b$, has to be added to the system, where $\hat{k} \approx \hat{k}_f$ as shown in Figure 11. Now we have:

$$G_{\bar{P}}(s) = \frac{s}{0.008s^2 + [1-(k_f - \hat{k}_f \hat{k}_u^{-1} k_u)R]s - (k_f - \hat{k}_f \hat{k}_u^{-1} k_u)/C}$$

Ideally when $\hat{k}_u^{-1} k_u = 1, \hat{k}_f = k_f$, the RHP pole will be canceled. However, due to the nonlinearity of k_f and k_u, and consider also pressure sensor dynamics. The perfect compensation is usually impossible. Either less compensation or over compensation will still downgrade the control performance.

7. Conclusions

This paper demonstrates the dynamics and fundamental control-oriented performance limitations inherent in the flow control unit. Modeling and identification of the FCV and the flow control unit in the ventilator are presented. The analysis shows that the achievable closed-loop bandwidth is considerably limited by the unexpected process zeros resulted form the valve exit manifold. On the other hand, due to the FCV has no outlet pressure balance, an unstable pole may be induced by patient circuit and results internal instability in the flow control unit.

The knowledge of the process zeros and poles serves as an important guideline for flow servo design. Examining the frequency response in Figure 4, it is also interested to notice that for a flow range around 10 to 40 LPM there is likely a second low frequency resonance moving between 20 to 40 Hz. To understand and remove these unwanted effects, further investigations on the dynamics of the downstream manifold and the dynamics interaction between the FCV and its exit manifold are needed. The instability problem may be solved by using the valve with outlet pressure balance.

Reference:

[1]. V. Szente & J Vad, "Computational and Experimental Investigation on Solenoid Valve Dynamics", Proceedings of 2001 IEEE/ASME International Conference on Advanced Intelligent Mechatronics, 8-12 July 2001, Como, Italy.

[2]. M. K. Zavarehi, P.D. Lawrence & F. Sassani, "Nonlinear Modeling and Validation of Solenoid-Controlled Pilot-Operated Servo valves", IEEE/ASME Transactions on Mechatronics, Vol. 4 No. 3, September 1999

[3]. B.W. Andersen, "The Analysis and Design of Pneumatic Systems".1967 by John Wiley & Sons, Inc.

[4]. J. Schoukens, R. Pintelon, and Y. Rolain, "Time domain identification, frequency domain identification. Equivalencies! Differences?", Proceeding of 2004 American Control Conference, Boston, MA. June30-July 2, 2004.

[5]. M, Borrello, "Controlling Respiratory Mechanical Impedance; An Analysis of Proportional Assist Ventilation". Proceeding of 2004 American Control Conference, Boston, MA. June30-July 2, 2004

[6]. S. Skogestad, and I. Postlethwaite, "Multivariable Feedback Control", John Wiley & Sons Ltd, 1996.